Nanobubbles at hydrophilic particle-water interfaces

Gang Pan[1*, 2], Guangzhi He[1], Meiyi Zhang[1], Qin Zhou[1], Tolek Tyliszczak[3], Renzhong Tai[4], Jinghua Guo[3], Lei Bi[1], Lei Wang[1], and Honggang Zhang[1]

1. Research Center for Eco-Environmental Sciences, Chinese Academy of Sciences, Beijing 100085, China.

2. School of Animal, Rural and Environmental Sciences, Nottingham Trent University, Brackenhurst Campus, NG25 0QF, UK

3. Advanced Light Source, Lawrence Berkeley National Laboratory, Berkeley, CA 94720, United States.

4. Shanghai Synchrotron Radiation Facility, Shanghai Institute of Applied Physics, Chinese Academy of Sciences, Shanghai 201204, China.

*Corresponding author. E-mail: gpan@rcees.ac.cn

Abstract: The puzzling persistence of nanobubbles breaks Laplace's law for bubbles, which is of great interest for promising applications in surface processing, H_2 and CO_2 storage, water treatment, and drug delivery. So far, nanobubbles are mostly reported on the hydrophobic planar substrates with atom flatness. It remains a challenge to quantify nanobubbles on rough and irregular surfaces due to the lack of characterization technique that can detect both the nanobubble morphology and chemical composition inside individual nanobubble-like objects. Here, by using synchrotron-based scanning transmission soft X-ray microscopy (STXM) with nanometer resolution, we discern nanoscopic gas bubbles > 25 nm with direct in-situ proof of O_2 inside the nanobubbles at a hydrophilic particle-water interface under ambient conditions. We find a stable cloud of O_2 nanobubbles at the diatomite particle-water interface hours after oxygen aeration and temperature variation. The in situ technique may be useful for many surface nanobubble related studies such as material preparation and property manipulation, phase equilibrium, nucleation kinetics and their relationships with chemical composition within the confined nanoscale space. The oxygen nanobubble clouds may be important in modifying particle-water interfaces and offering breakthrough technologies for oxygen delivery in sediment and/or deep water environment.

Introduction

Observations of nanobubbles on hydrophobic planar substrates have attracted much attention,[1, 2, 3, 4, 5] however, it is not clear whether they can form and persist on rough and fully wetted (i.e., hydrophilic) surfaces under ambient conditions.[6, 7, 8, 9] If the remarkable stability (hours and days) of nanobubbles is universally true, [10, 11, 12] something is evidently missing in the existing theory, since the small curvature radius implies a high Laplace pressure inside the nanobubbles that should drive the bubbles dissolution in the liquid instantly (~1 μs).[13, 14] Studies of interfacial nanobubbles may provide new insights not only in gas-liquid-solid equilibria at nanoscale, but also in efficient and environmental friendly nanotechnologies.[15] Nanoscopic gaseous bubbles can be eventually dissolved in the bulk environment without any toxic effects commonly related to conventional solid nanomaterials.[16]

Atomic force microscopy (AFM) and direct optical visualization are currently the main methods for investigating interfacial nanobubbles,[6, 17, 18, 19] but they cannot detect the identity and the composition of the nanoscale objects. Elemental and chemical analysis combined with high-resolution imaging has been a key requirement for fully characterizing nanobubbles. Such an effort has been attempted using AFM followed by attenuated total reflection infrared spectrum (ATR-IR), by which the existence of CO_2 nanobubbles at the hydrophobic silicon wafer-water interface was found.[2, 20] However, the image and chemical information have to be measured separately from two different samples (i.e., ex situ), which are prepared specifically for the two instruments. Moreover, homonuclear diatomic molecules such as N_2 and O_2, and inert gases are not infrared active, so they are often undetectable by ATR-IR spectroscopy. The AFM-based characterization requires the substrates with high flatness, which is inaccessible for irregular or porous particle-water interfaces that are ubiquitous in the environment. It is anticipated that studies on the physicochemical properties of nanobubbles, such as phase equilibrium, nucleation kinetics and their relationships with chemical composition, will become a challenging and exciting direction in the near future. An in situ experimental technique which can simultaneously resolve the nanoscale morphologies and the chemical composition inside the

nanobubble-like objects (i.e., distinguish nanobubbles from other objects) at various interfaces is of fundamental significance for studying these properties of nanobubbles.

Synchrotron-based scanning transmission X-ray microscopy (STXM) can simultaneously provide nanometre-resolved maps and elemental information for target objects under in situ conditions.[21, 22, 23] STXM imaging has been used to visualize the micro- and nanobubbles of SF_6 and Ne, but the chemical information inside the bubbles has not been obtained due to the limitation of the instrument.[23]

Here, we use STXM to explore the O_2 nanobubbles at a hydrophilic particle-water interface. The chemical composition of the nanobubbles is analyzed by means of near-edge X-ray absorption fine structure (NEXAFS) spectra. NEXAFS spectroscopy probes the excitation of core electron by X-ray into unoccupied molecular orbitals and provides element-specific information.[24, 25] We prepare an O_2-aerated diatomite ($SiO_2 \cdot nH_2O$, a hydrophilic siliceous material which is widespread in natural environments[26]) suspension as the model system. Surface nanobubbles were generated using temperature variation.[14, 27] The stability of O_2 nanobubbles on the hydrophilic particles was investigated hours after oxygen aeration.

Methods

Materials and sample preparation. A diatomite (analytical grade, Beijing Chemical Regents Co.)-water suspension (0.55 g/L, 100 mL glass beaker) was aerated with pure O_2 (99.99%) in an ice-water bath under ambient pressure for 1 h. The control sample (an unaerated diatomite suspension) was prepared by the same operation as above, except for lack of O_2 aeration. The mixture was centrifugated for 15 min at a relative centrifugal force of 2240 g (5000 rpm) to remove large particles from solution, and then the supernatant was extracted and subjected to STXM measurements at ambient temperature of 25 °C. The ice-water bath was used to enhance the dissolved O_2 level in the solution, and the temperature-increasing operation was carried out to generate oxygen bubbles at the solid-liquid interfaces.[14, 27] A small contact angle of water on the diatomite (17º, JY-PHb, Jinhe Co.) showed that the diatomite was highly hydrophilic. BET surface area analysis indicated a specific surface area of 7.4

m^2/g (ASAP-2010, Micromeritics) for the diatomite. The particle-size distribution, measured with a Mastersizer 2000 analyzer (Malvern, UK), ranged from 0.4 to 5.5 μm. The volume average particle diameter was 3.67 μm. All solutions were produced in ultrapure water (resistivity 18MΩ.cm).

In situ STXM measurement and data treatment. STXM experiment was carried out on the beamline 11.0.2 at the Advanced Light Source (ALS) in Lawrence Berkeley National Laboratory. The STXM instrument at ALS provides images with a spatial resolution of ~25 nm and an energy resolution (E/ΔE) of 2500-7500 for X-ray photons of 200-2000 eV (~0.08 eV at O K-edge). The STXM chamber was filled with 760 Torr He prior to sample measurements. A droplet (water or suspension, ~2 μL) was placed on a 5 mm × 5 mm Si wafer with 0.5 mm × 0.5 mm opening of 100-nm-thick Si_3N_4 membrane, and covered with another Si_3N_4 membrane. The borders of the Si_3N_4 sandwich were sealed using epoxy. Then the resulting wet cell was loaded into the sample holder in the STXM chamber after the glue solidify. The wet cell was measured from the optical microscope by counting the interference fringes. The O_2 spectrum was recorded as the partial pressure of oxygen gas was 2 Torr in the STXM chamber. For measurements of the spectrum of water vapor, the STXM chamber was opened to a flask with water till the partial pressure of water vapor inside the chamber was 2 Torr.

The monochromatic X-ray beam was focused to a spot size of 25 nm in diameter using a Fresnel zone plate, and the sample was then raster-scanned at the focal point through detecting the transmitted X-ray flux. The transmitted X-ray intensity was recorded using a scintillator and photomultiplier tube and measured as a function of photon energy and position. The recorded transmitted X-ray intensity (I) of the samples was normalized by the incident intensity (I_0) to convert to the optical density (absorbance) $OD = -\ln(I/I_0)$. Image stacks were obtained by scanning the sample in the x–y directions of selected areas with a step increment of 0.2 eV over the energy range of 525.0–555.0 eV. After spatially aligning the stack, principle component analysis (PCA) was used to obtain the primary components in the data set. Subsequently, a cluster analysis (CA) was performed to group pixels (i.e., classify areas in the sample) according to statistical similarities in their spectra.[21, 28] The STXM data were processed using

103 the aXis2000 software package (available from http://unicorn.mcmaster.ca/aXis2000.html).

104 ## Results and discussion

105 The O K-edge NEXAFS spectra of oxygen gas, water vapor, and liquid water are presented in Figure 1,
106 which are in good agreement with literatures.[22, 24, 29, 30, 31] The NEXAFS of oxygen gas is characterized
107 by a strong resonance at 531.2 eV and a weak broad absorption feature in the energy range of 537-545
108 eV. The broad absorption band is due to the 1s→ σ* transition, while the strong resonance (nearly
109 fivefold the intensity of σ* region) is attributed to the 1s→ π* transition.[24] By taking advantage of the
110 distinct strong absorption feature, the π* signature at ~531 eV can be used as a clear indicator of the
111 presence of O_2 in a well-controlled system.[31, 32]

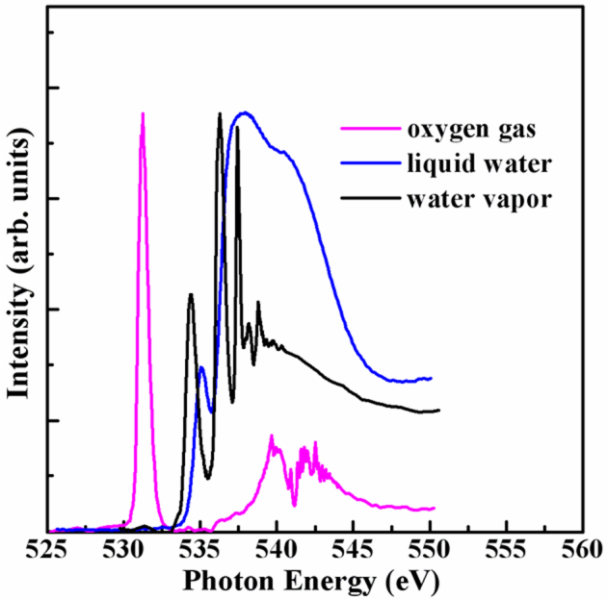

112

113 **Figure 1.** O K-edge NEXAFS spectra of oxygen gas, liquid water and water vapor.

114 To explore the O_2 nanobubbles at hydrophilic particle surfaces, two diatomite suspension samples
115 are prepared by the same procedure, except for the pure O_2 (99.99%) aeration process. A STXM image
116 of the unaerated diatomite suspension is shown in Figure 2a. The dark and pale grey shades are due to
117 the different transmitted intensities, and the particle regions (dark grey) within the suspension become
118 visible. Absorption spectra extracted from the water medium and solid regions are compared in Figure
119 2b. The spectrum from water phase shows essentially the same shape as the pure liquid water (see

Figure 1), which consists of three main regions: the pre-edge (around 535 eV), the main edge (537 to 538 eV), and the post-edge (540 to 541 eV).[29] The NEXAFS of the solid region is consistent with the characteristics of SiO_2, which is characterized by a weak π* resonance at ~532 eV and a high σ* resonance in the energy range of 535-545 eV.[22] The difference between the spectra of diatomite and water phase (Figure 2b inset) also does not show any significant spectral features of oxygen gas. Therefore, no signal of oxygen gas is observed in the unaerated diatomite suspension sample.

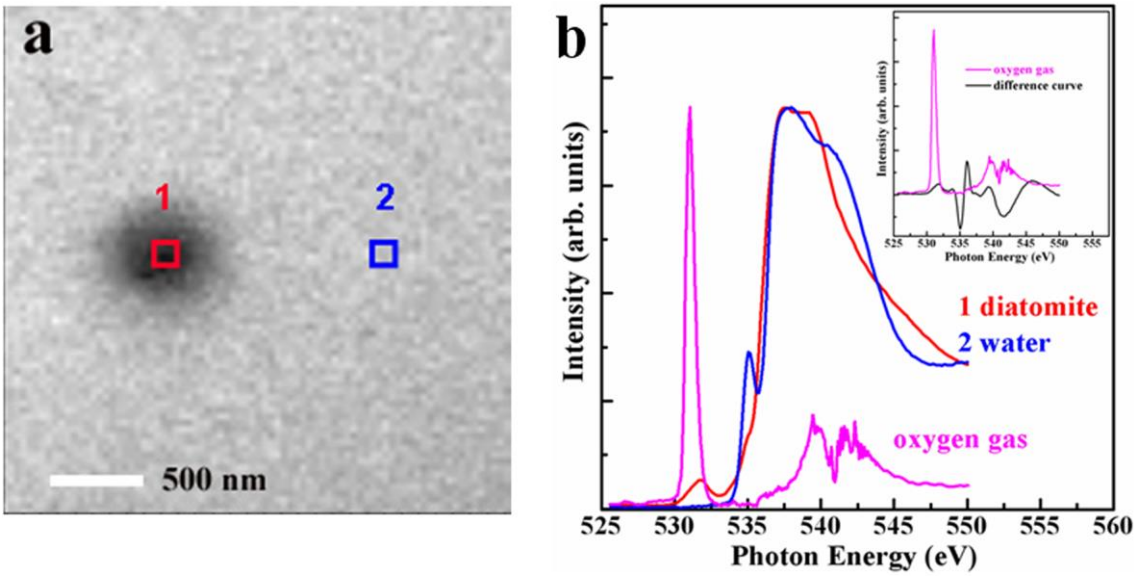

Figure 2. STXM image and X-ray absorption spectra of unaerated diatomite suspension. (a) STXM image recorded at 539.2 eV. (b) O K-edge NEXAFS spectra taken from the regions shown in (a). Inset, the difference spectrum obtained by subtracting the blue curve from the red one.

The STXM image of diatomite suspension after 1 h O_2 aeration is presented in Figure 3a. Chemical contrast map of the sampling region (Figure 3b) is obtained by principle component analysis and cluster analysis (PCA-CA) of all NEXAFS spectra for each pixel.[21] The PCA-CA analysis identifies four chemically distinct regions within the O_2-aerated suspension which exhibit different NEXAFS spectra in Figure 3c. The blue pixels represent the water phase. The spectrum extracted from the O_2-aerated water phase shows spectral features nearly identical to those of unaerated water (Figure 2b), except for a small absorption feature at around 531 eV (see the blue line in Figure 3c), suggesting that the O_2 saturation

level in water phase has been increased to the extent that is detectable for the STXM measurement after 1 h O_2 aeration and temperature enhancement. The intensity ratio of the π* resonance (at 531.2 eV) to the σ* resonance (at around 538 eV) of the NEXAFS spectra taken from the region on and around the particle is significantly higher than those of diatomite and water (see Figure 2b), which indicates the existence of O_2 at the particle-water interface. The high spatial resolution of STXM mapping allows us to discern the individual O_2-filled nanobubbles with diameters down to 25 nm (see the colored spots in Figure 3b, typically 25-50 nm), as well as a cloud of O_2 nanobubbles around the diatomite particles. The nanoscale density-gradient pattern of O_2 surrounding the water-dispersed particle obtained from the cluster map indicates that the O_2 content within the nanobubbles at the diatomite-water interface may vary to a large extent. The intensity of π* resonance increases significantly from bulk water to solid surfaces (Figure 3c), indicating the accumulation of O_2 near the particle surfaces. The weak σ* resonance feature of oxygen gas (approximately one fifth of the intensity of π* resonance) is not directly observed, which may be overwhelmed by the strong absorption band originating from dense water and solid phases (see the difference between the green and blue spectra in Figure 3c inset, which shows a similar spectral profile as O_2 spectrum).

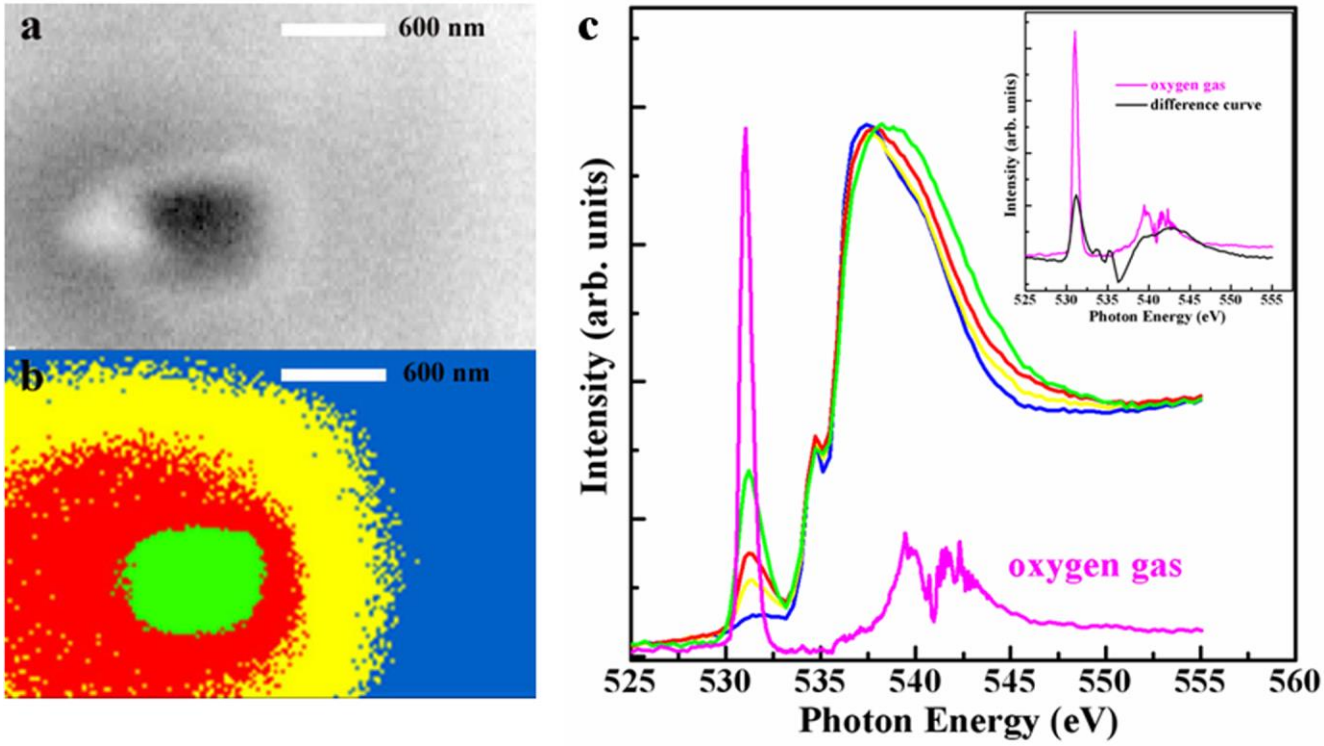

Figure 3. Characterization of O_2-aerated diatomite suspension. (a) STXM image recorded at 538.5 eV. (b) Cluster map of the sampling region. (c) O K-edge NEXAFS spectra corresponding to the clusters shown in (b) and O_2 reference. Inset, the difference spectrum obtained by subtracting the blue curve from the green one.

Our findings indicate that the surfaces of water-dispersed particles can be decorated by a stable nanoscale gas phase through simple aeration and temperature variation. Phil Attard reported that the nanobubbles could form from a solution supersaturating with air and were stable on hydrophobic surfaces.[33] Our results further prove that solution supersaturating is a necessary condition for the formation of nanobubbles, and the nanobubbles can also exist on hydrophilic surfaces. Gas supersaturated in solution and temperature fluctuation happen frequently in the nature, the existence of nanobubbles on the particle-water interface may be a common phenomenon. There are many kinds of water-dispersed micro/nano particles in nature, such as enzyme, microorganism, cells and mineral particles and so on. Many interface behaviors or biochemical processes, adsorption/desorption, dissolution/precipitation, dispersion/aggregation, ion exchange, interfacial electron transfer, catalysis,

would be changed or became different in the presence of nano cloud around the particles. This finding could open new avenues for exploring these unclear interfacial behaviors in many research fields.

On the other hand, the persistence of nanobubbles clouds at particle-water interface may open novel environmental and aquatic engineering applications. O_2-filled nanobubbles loaded on macroscopic particles of clay or soil can be purposely delivered to polluted water and especially anoxic sediment, and efficiently revive the polluted natural waters.[34, 35, 36] The hypoxia and anoxia problem in deep water is an extremely difficult problem to be tackled by conventional technologies such as areation and ventilation[37]. The O_2 nanobubble materials may lift the bottleneck problems of safety, cost, and performance of nanomaterials for the remediation of anoxia and eutrophication in aquatic environment.[15] The 'window period' triggered by O_2 nanobubble materials and the triggered physic-chemical and microbial responses may greatly change the sediment-water proceses, which will in turn affect the air-water exchange of green house gases. The STXM method developed here may greatly facilitate nanobubble related studies on environmental samples.

Conclusions

We observe nanoscopic gas bubbles > 25 nm with direct proof of O_2 inside the nanobubbles at a hydrophilic particle-water interface under ambient conditions by using scanning transmission X-ray microscopy. We find a stable cloud of O_2 nanobubbles at the diatomite particle-water interface hours (at least 4 hours for the whole STXM experiment process) after oxygen aeration and temperature treatment. STXM is a promising technique for studying the nanobubbles nucleation process near the solid/water interfaces at irregular and rough surfaces. The persistence of nanoscopic gases at a fully wetted hydrophilic surface prompts the need to further explore the nature of gas-liquid-solid equilibria at nanoscale and to extent the nanobubbles application.

Acknowledgements

We are grateful to Philip Ball for valuable comments and suggestions on the manuscript. We thank

SSRF for performing preliminary STXM experiments and helpful assistance in this study. This work is supported by the Strategic Priority Research Program of the Chinese Academy of Sciences (XDA09030203) and the National Basic Research Program of China (2010CB933600). The Advanced Light Source is supported by the U.S. Department of Energy under Contract No. DE-AC02-05CH11231.

References

1. Tyrrell, J. W. G.; Attard, P. Images of nanobubbles on hydrophobic surfaces and their interactions. *Phys. Rev. Lett.* **2001,** *87* (17), 176104.
2. Zhang, X. H.; Khan, A.; Ducker, W. A. A nanoscale gas state. *Phys. Rev. Lett.* **2007,** *98* (13), 136101.
3. Zhang, X.; Lhuissier, H.; Sun, C.; Lohse, D. Surface nanobubbles nucleate microdroplets. *Phys. Rev. Lett.* **2014,** *112* (14), 144503.
4. Peng, H.; Birkett, G. R.; Nguyen, A. V. Progress on the Surface Nanobubble Story: What is in the bubble? Why does it exist? *Advances in colloid and interface science* **2014**.
5. Lohse, D.; Zhang, X. H. Surface nanobubbles and nanodroplets. *Rev. Mod. Phys.* **2015,** *87* (3), 981-1035.
6. Seddon, J. R. T.; Lohse, D. Nanobubbles and micropancakes: gaseous domains on immersed substrates. *J. Phys.-Condes. Matter* **2011,** *23* (13), 133001.
7. Liu, Y.; Wang, J.; Zhang, X.; Wang, W. Contact line pinning and the relationship between nanobubbles and substrates. *J. Chem. Phys.* **2014,** *140* (5), 054705.
8. Zhang, X. H.; Zhang, X. D.; Lou, S. T.; Zhang, Z. X.; Sun, J. L.; Hu, J. Degassing and temperature effects on the formation of nanobubbles at the mica/water interface. *Langmuir* **2004,** *20* (9), 3813-3815.
9. Pan, G.; Yang, B. Effect of surface hydrophobicity on the formation and stability of oxygen nanobubbles. *Chemphyschem* **2012,** *13* (8), 2205-2212.
10. Zhang, X. H.; Quinn, A.; Ducker, W. A. Nanobubbles at the interface between water and a hydrophobic solid. *Langmuir* **2008,** *24* (9), 4756-4764.
11. Weijs, J. H.; Lohse, D. Why surface nanobubbles live for hours. *Phys. Rev. Lett.* **2013,** *110* (5), 054501.
12. Borkent, B. M.; Dammer, S. M.; Schoenherr, H.; Vancso, G. J.; Lohse, D. Superstability of surface nanobubbles. *Phys. Rev. Lett.* **2007,** *98* (20).
13. Ball, P. Nanobubbles are not a superficial matter. *ChemPhysChem* **2012,** *13* (8), 2173-2177.
14. Seddon, J. R. T.; Kooij, E. S.; Poelsema, B.; Zandvliet, H. J. W.; Lohse, D. Surface bubble nucleation stability. *Physical Review Letters* **2011,** *106* (5), 056101.
15. Brooks, M. Impossibubbles. *New Scientist* **2012,** *215* (2872), 38-41.
16. Masciangioli, T.; Zhang, W. X. Environmental technologies at the nanoscale. *Environ. Sci. Technol.* **2003,** *37* (5), 102A-108A.
17. Karpitschka, S.; Dietrich, E.; Seddon, J. R. T.; Zandvliet, H. J. W.; Lohse, D.; Riegler, H. Nonintrusive optical visualization of surface nanobubbles. *Phys. Rev. Lett.* **2012,** *109* (6), 066102.
18. Chan, C. U.; Ohl, C.-D. Total-internal-reflection-fluorescence microscopy for the study of nanobubble dynamics. *Phys. Rev. Lett.* **2012,** *109* (17), 174501.
19. Walczyk, W.; Schoenherr, H. Characterization of the Interaction between AFM Tips and Surface Nanobubbles. *Langmuir* **2014,** *30* (24), 7112-7126.

20. German, S. R.; Wu, X.; An, H.; Craig, V. S. J.; Mega, T. L.; Zhang, X. Interfacial nanobubbles are leaky: permeability of the gas/water interface. *ACS Nano* **2014,** *8* (6), 6193-6201.
21. Lehmann, J.; Solomon, D.; Kinyangi, J.; Dathe, L.; Wirick, S.; Jacobsen, C. Spatial complexity of soil organic matter forms at nanometre scales. *Nat. Geosci.* **2008,** *1* (4), 238-242.
22. de Smit, E.; Swart, I.; Creemer, J. F.; Hoveling, G. H.; Gilles, M. K.; Tyliszczak, T.; Kooyman, P. J.; Zandbergen, H. W.; Morin, C.; Weckhuysen, B. M.; de Groot, F. M. F. Nanoscale chemical imaging of a working catalyst by scanning transmission X-ray microscopy. *Nature* **2008,** *456* (7219), 222-225.
23. Zhang, L.; Zhao, B.; Xue, L.; Guo, Z.; Dong, Y.; Fang, H.; Tai, R.; Hu, J. Imaging interfacial micro- and nano-bubbles by scanning transmission soft X-ray microscopy. *J. Synchrot. Radiat.* **2013,** *20*, 413-418.
24. Stöhr, J. *NEXAFS Spectroscopy*; Springer: Berlin, 1992; Vol. 25.
25. He, G. Z.; Pan, G.; Zhang, M. Y.; Wu, Z. Y. Quantitative XANES Studies on Metastable Equilibrium Adsorption of Arsenate on TiO2 Surfaces. *J. Phys. Chem. C* **2009,** *113* (39), 17076-17081.
26. Zhong, S. H.; Li, C. F.; Xiao, X. F. Preparation and characterization of polyimide-silica hybrid membranes on kieselguhr-mullite supports. *J. Membr. Sci.* **2002,** *199* (1-2), 53-58.
27. Yang, S.; Dammer, S. M.; Bremond, N.; Zandvliet, H. J. W.; Kooij, E. S.; Lohse, D. Characterization of nanobubbles on hydrophobic surfaces in water. *Langmuir* **2007,** *23* (13), 7072-7077.
28. Lerotic, M.; Jacobsen, C.; Schafer, T.; Vogt, S. Cluster analysis of soft X-ray spectromicroscopy data. *Ultramicroscopy* **2004,** *100* (1-2), 35-57.
29. Wernet, P.; Nordlund, D.; Bergmann, U.; Cavalleri, M.; Odelius, M.; Ogasawara, H.; Naslund, L. A.; Hirsch, T. K.; Ojamae, L.; Glatzel, P.; Pettersson, L. G. M.; Nilsson, A. The structure of the first coordination shell in liquid water. *Science* **2004,** *304* (5673), 995-999.
30. Myneni, S.; Luo, Y.; Naslund, L. A.; Cavalleri, M.; Ojamae, L.; Ogasawara, H.; Pelmenschikov, A.; Wernet, P.; Vaterlein, P.; Heske, C.; Hussain, Z.; Pettersson, L. G. M.; Nilsson, A. Spectroscopic probing of local hydrogen-bonding structures in liquid water. *J. Phys.-Condes. Matter* **2002,** *14* (8), L213-L219.
31. Wurth, W.; Stohr, J.; Feulner, P.; Pan, X.; Bauchspiess, K. R.; Baba, Y.; Hudel, E.; Rocker, G.; Menzel, D. Bonding, structure, and magnetism of physisorbed and chemisorbed O_2 on Pt(111). *Phys. Rev. Lett.* **1990,** *65* (19), 2426-2429.
32. Bukhtiyarov, V. I.; Havecker, M.; Kaichev, V. V.; Knop-Gericke, A.; Mayer, R. W.; Schlogl, R. X-ray absorption and photoemission studies of the active oxygen for ethylene epoxidation over silver. *Catal. Lett.* **2001,** *74* (3-4), 121-125.
33. Attard, P.; Moody, M. P.; Tyrrell, J. W. G. Nanobubbles: the big picture. *Physica A: Statistical Mechanics and its Applications* **2002,** *314* (1–4), 696-705.
34. Pan, G.; Dai, L. C.; Li, L.; He, L. C.; Li, H.; Bi, L.; Gulati, R. D. Reducing the recruitment of sedimented algae and nutrient release into the overlying water using modified soil/sand flocculation-capping in eutrophic lakes. *Environ. Sci. Technol.* **2012,** *46* (9), 5077-5084.
35. Pan, G.; Yang, B.; Wang, D.; Chen, H.; Tian, B. H.; Zhang, M. L.; Yuan, X. Z.; Chen, J. A. In-lake algal bloom removal and submerged vegetation restoration using modified local soils. *Ecol Eng* **2011,** *37* (2), 302-308.
36. Pan, G.; Chen, J.; Anderson, D. M. Modified local sands for the mitigation of harmful algal blooms. *Harmful Algae* **2011,** *10* (4), 381-387.
37. Conley, D. J. Save the Baltic Sea. *Nature* **2012,** *486* (7404), 463-464.

278 **TOC Graphic**

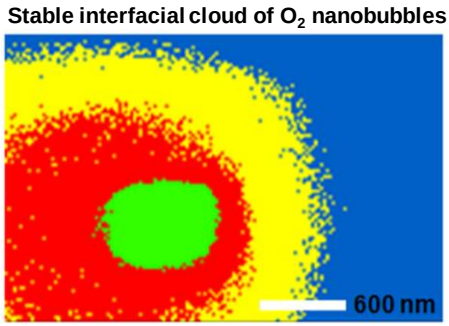

279